Received: 30 March 2021 | Revised: 28 July 2021 | Accepted: 31 July 2021

DOI: 10.1002/app.51515

ARTICLE

Applied Polymer SCIENCE WILEY

Improving gas barrier properties of sugarcane-based LLDPE with cellulose nanocrystals

Madhumitha Natarajan[1] | **Ronald C. Sabo**[2] | **Nicole M. Stark**[1,2] | **Laurent M. Matuana**[1]

[1]School of Packaging, Michigan State University, East Lansing, Michigan, USA

[2]U.S. Department of Agriculture, Forest Service, Forest Products Laboratory, One Gifford Pinchot Drive, Madison, Wisconsin, USA

Correspondence
Laurent M. Matuana, School of Packaging, Michigan State University, East Lansing, MI 48824, USA.
Email: matuana@msu.edu

Funding information
Mcintire-Stennis, Grant/Award Number: 1017725

Abstract

This study was aimed at improving the gas barrier property of sugarcane based LLDPE using cellulose nanocrystals (CNCs). Specifically, this study evaluated the effect of CNC content on the crystallinity, tortuosity factor, carbon dioxide permeability (P_{CO2}), and/or oxygen permeability (P_{O2}) of bio-LLDPE sheets and films. All nanocomposites showed considerable improvement in gas barrier irrespective of the CNC content. The P_{CO2} coefficient of LLDPE sheets decreased by 36% by adding 10 wt% of CNCs into the sheet. Similarly, a significant decline in both P_{O2} (about 50%) and P_{CO2} (about 33%) coefficients of LLDPE films was obtained by adding 2.5 wt% of CNCs into the films. Nevertheless, no correlation was established between gas permeability and percent crystallinity of LLDPE sheet since the P_{CO2} coefficient decreased almost linearly with increasing CNC content whereas the percent crystallinity of LLDPE increased only up to 2.5% CNC content and remained constant thereafter. In contrast, the tortuosity factors calculated from the gas diffusion coefficients increased almost linearly with CNC contents and correlated well with the gas permeability improvement in bio-LLDPE-based nanocomposites. Consequently, the enhanced gas barrier in the nanocomposite was assigned to the tortuosity effect created by the impermeable CNCs rather than the changes in percent crystallinity.

KEYWORDS

biopolymers and renewable polymers, cellulose and other wood products, composites, films, packaging

1 | INTRODUCTION

Most of the plastics used in the industry for various applications including packaging applications are petroleum-based and are obtained from crude oil. However, the use of petroleum-based plastics is a major contributor to global greenhouse gas emissions.[1] Therefore, there is a need for more sustainable, environmentally friendly alternatives like biobased and/or biodegradable polymers.[2] Bioplastics have a smaller carbon footprint compared to petroleum-based plastics.[3] In addition to being sustainable, biobased plastics also have physico-mechanical properties like petroleum-based polymers; and hence are ideal alternative to the latter.[4] Globally, bioplastics contribute to about 5.4 tons of all the plastics currently in the market and are expected to grow by 20% by the year 2024.[5] The recent development of sugarcane-based polyethylene is a typical example of more environmentally sustainable plastics. Recently, Braskem, a

Brazilian chemical company, has launched a set of biobased polyethylene derived from sugarcane ethanol that have similar properties to their petroleum-based counterparts.

Polyethylene (PE) is one of the most widely used polymers in the plastics industry and has different variants like high density polyethylene (HDPE), low density polyethylene (LDPE) and linear low-density polyethylene (LLDPE). Each variant has its unique properties in terms of appearance, crystallinity, mechanical, and barrier properties. In food packaging, material with transparency is highly desired as it influences packaging aesthetics along with material having good moisture and gas barrier to provide required shelf life for the packaged product. All PE variants have good water barrier but poor gas barrier, and their transparencies vary based on the density of the PE used and the thickness of the material used for packaging.[6–8]

HDPE has good gas barrier compared to other variants of PE but has a milky white appearance, whereas LDPE has poor gas barrier but has excellent transparency. Since both properties are crucial for packaging applications these drawbacks limit the scope of these polymers in packaging. LLDPE on the other hand has improved regularity in its structure, and depending on its density, could be better than LDPE in most properties, especially in terms of its gas barrier properties. LLDPE is also transparent in appearance making it better than HDPE in terms of transparency. Consequently, LLDPE is a suitable polymer for applications requiring both good transparency and good gas barrier like produce bags, frozen food bags, as a protective pallet stretch film, etc.[7–10] However, when compared to other plastics like EVOH, PET, and so on, LLDPE is poor in its gas barrier properties. Further enhancement in gas barrier properties will make it more suitable for a wide range of packaging applications.

Various methods are commonly employed to enhance the gas barrier properties of packaging materials. Coating as well as production of multilayers and laminates structures are few techniques where layers of different materials are combined to achieve desired gas barrier properties of the films.[11,12] Unfortunately, these different layers cannot be easily separated at the end of the material's lifecycle, which leads to problems with recyclability and often a lot of these multilayer films end up in the landfill. Landfill is a major issue with polymers as it is an unsustainable waste management practice.

Manufacture of bio-based composite films of monolayer structure with excellent gas barrier properties could be the solution to a such problems as they are just as recyclable as their neat polymer counterparts.[13] Monolayered nanocomposite films manufactured by incorporating nanoparticles such as nano clay,[14] cellulose whiskers,[15] cellulose nanofibers (CNFs),[16] cellulose nanocrystals (CNCs),[17–19] and so on into various polymer matrices have been reported to improve the gas barrier properties of the neat polymer counterparts. The improved barrier performance of nanocomposite films has been mainly assigned to the tortuosity effect created by the presence of highly crystalline nanoparticles into the polymeric matrix, which increases the degree of crystallinity of the neat polymer. These crystals increase the effective travel path length for permeants diffusing through the nanocomposites. This reduces the rate of diffusion, thus lowering permeation as reported by others.[17–19] Unfortunately, limited work has been done on nanocomposites based on bio-PE. Recently, Bazan and coworkers investigated the mechanical, thermal properties, and micromechanics of composites made of biobased polyethylene and a combination of natural fibers (e.g., wood flour, coconut shell fibers, and basalt fibers). They reported that hybridization of cellulose fibers with basalt fibers significantly improves the properties compared to adding cellulose fibers alone. Additionally, the accelerated water and thermal aging of composites samples deteriorated their strength properties compared to unaged counterparts.[6]

It is well accepted that gas barrier properties of semicrystalline polymer filled with nanoparticles is affected not only by the impermeable nanoparticles, but also greatly depends on its crystallinity and crystalline morphology.[15–21] Although a negative correlation between percent crystallinity and permeability coefficients of various permeants has been reported for nanocomposites,[15–21] polymer crystallinity is certainly not the only factor influencing its permeability, since no correlation has also been established between level of crystallinity and permeability.[22–24] For example, despite a 27% reduction in crystallinity, the oxygen and carbon dioxide permeability of the polypropylene (PP)/ethylene-propylene-diene rubber (EPDM) blend nanocomposite reduced two-fold by adding only 1.5 vol% montmorillonite-based organoclay into PP/EPDM blend.[22] The increase in barrier property of the nanocomposite blend was attributed to the combination of two phenomena, including (i) the decrease in area available for diffusion, a result of impermeable flakes replacing permeable polymer; and (ii) the increase in the distance a solute must travel to cross the film as it follows a tortuous path around the impermeable flakes.[22] Similarly, a significant decline in both O_2 (about 45%) and CO_2 (about 68%) permeability coefficients of PLA films was obtained by adding 1.37 vol% graphene oxide nanosheets (GONSs) into PLA film, even though all the PLA nanocomposite films were basically amorphous.[23] This large improvement in gas barrier properties of PLA/GONSs nanocomposite film was mainly assigned to the impermeable GONSs acting as crystallites and the strong interfacial adhesion between GONSs

and PLA matrix, rather than the changes in crystallinity and crystalline morphology of PLA matrix.[23] Therefore, in addition to level of crystallinity, the role of other factors contributing to barrier improvement like the tortuosity factor must also be investigated to understand the mechanisms of barrier improvement in nanocomposites.

Therefore, this study was aimed at improving the gas barrier property of sugarcane based LLDPE films using cellulose nanocrystals (CNCs). Specifically, this study evaluated the effect of CNC content on gas barrier properties of sugarcane based LLDPE sheets and films. Emphasis was placed on the gravimetric-sorption method to quantify the diffusion and solubility coefficients needed to estimate the tortuosity factor and permeability coefficient, which were correlated to elucidate the mechanism involved in barrier property improvement in nanocomposites.

2 | EXPERIMENTAL

2.1 | Materials

Sugarcane-based LDPE (STN7006), LLDPE (SLH118), and HDPE (SGD4960) obtained from Braskem Petrochemical (Sao Paulo, State of Sao Paulo, Brazil) were used as polymer matrices. Their respective melt flow indices were 0.6, 1, and 0.7 g/10 min, whereas their respective densities were 0.924, 0.916, and 0.962 g/cm^3. The biobased content of the polymers was 95%, 84%, and 96% for LDPE, LLDPE, and HDPE, respectively. The CNCs (2018-FPL-CNC-126) used in this study were produced in the Forest Products laboratory's pilot plant in Madison, WI. Sulfuric acid hydrolysis was used to produce freeze dried cellulose nanocrystals around 100–300 nm long and a diameter of around 5 nm.[25] Sulfuric acid, PC (printed circuit) grade, was supplied by Columbus Chemical Industries, Inc. (Columbus, WI) at 64% by weight. CNCs were processed in a high intensity mixer (MX1050XTS from Waring Commercial Xtreme) for 1 min at 22,000 rpm to reduce the fiber agglomeration and then oven-dried for at least 24 h to remove any absorbed moisture.

2.2 | Samples manufacture for permeability tests

Two types of barrier measurement techniques were used in this study to understand the mechanism of gas barrier improvement in bio-LLDPE/CNC nanocomposites. The first approach included the gravimetric/sorption method, which measures the amount of gas uptake or lost from the sample. This method required rigid samples of approximately 1.5 to 2 mm thick for performing the tests effectively, which were prepared using compression molding process.[26,27] The second technique involved the isostatic permeability method, which measures the gas transmission rate through the sample and estimates its permeability coefficient. This method required thin film samples for tests to be performed effectively, these were prepared using blown film extrusion. Karkhanis et al performed isostatic method of permeability measurement successfully for their PLA/CNC nanocomposites using similar sample preparation techniques.[17]

2.2.1 | Compression molded samples for gravimetric-sorption method

The bio-LLDPE pellets along with dried CNCs were blended in a 60 ml electrically heated three-piece internal mixer/measuring head (3:2 gear ratios) with counter-rotating roller style mixing blades (C.W. Brabender Instruments, Inc.). The mixer was driven by a 7.5 hp Intelli-Torque Plasti-Corder Torque Rheometer® (C. W. Brabender Instruments, Inc.). The polymer and CNC were mixed for 3 min at 170 C. The rotor speed used was 35 rpm and weight charge set at 45 g determined from the preliminary testing. The CNCs contents in the nanocomposites were fixed at 2.5%, 5%, 7.5%, 10%, and 13.5% of total material weight. A 5 kg dead weight was put on the top of the ram throughout the experiments.[26,27] The blended materials were cooled and pressed at 180 C and 5 tons of maximum pressure for 6 min using the hydraulic laboratory press (Carver, Model 120-10HC) to a target thickness of 2 mm using a metal spacer while processing. Similar process was utilized to manufacture control samples based on neat LLDPE, neat LDPE, and neat HDPE.

2.2.2 | Blown film extrusion for Isostatic permeability method

Bio-LLDPE pellets and dried CNCs were blended for 1 min at high intensity setting in a commercial blender (MX1050XTS from Waring Commercial Xtreme). The blended materials were blown into films using a 19 mm single-screw extruder (C.W. Brabender Instruments, South Hackensack, NJ) with a length-to-diameter ratio of 30:1 as previously described.[17,19,28] The annular die used was of 25.4 mm in diameter and a die-opening of 0.889 mm. The temperature profile of the extruder was set to 185–185–185–185 C from the hopper to die. The speeds of the extruder rotational screw and take up rollers were both set to 20 rpm, while an air pressure of 0.207 kPa (0.030 psi) was used to inflate the film to a

blow-up ratio of 3, leading to ~0.062 mm thick films, measured by digital micrometer (model 49–70 from TMI, Ronkonkoma, NY).[17,19,28]

3 | PROPERTY EVALUATION

3.1 | Gas permeability by sorption experiments

The desorption experiments were performed according to the gravimetric method used in previous research work.[26,27] Compression molded samples were cut into 0.5″ 1″ rectangular specimens. The samples were weighed using a four-digit precision digital balance, their thickness measured, and they were placed in a chamber that was later pressurized with carbon dioxide (CO_2) at 800 psi and room temperature. The samples were left in the chamber until they were saturated with CO_2 (minimum of 16 h). At the end of the saturation, the CO_2-saturated samples were removed from the pressure chamber and weighed again on the balance to determine the amount of CO_2 absorbed or measured solubility. And the solubility coefficient (S) was calculated as follows[29,30]:

$$S = \frac{C_i}{p_i} \tag{1}$$

where p_i is the partial pressure of gas and C_i is the solubility of the gas in polymer given by the formula:

$$C_i = \frac{W_{tgas}}{V_p} \tag{2}$$

with W_{tgas} as the weight of the dissolved gas per unit volume of polymer (V_p).

Once the percent weight gain of CO_2 was recorded, desorption process was carried out immediately to determine the amount of gas lost at regular time intervals and estimate the diffusivity of gas (D) in the sample, which is given by the following equation[26,27,29]:

$$D = \frac{\pi}{16}\left[\frac{d\frac{M_t}{M_\infty}}{d\frac{\sqrt{t}}{l}}\right]^2 \tag{3}$$

where M_∞ is the mass uptake at infinite time, M_t is the amount of gas uptake or lost at time t and l is the average sample thickness. If a curve is plotted for $\frac{M_t}{M_\infty}$ versus $\frac{\sqrt{t}}{l}$, the initial gradient of the curve can also be used to calculate the value of diffusion coefficient (D). Experimentally for a system in which the diffusion coefficient is constant, if the half time for desorption or absorption is observed, the value of this constant can be given by[26,27,29]:

$$D = \frac{0.049}{\left(\frac{\sqrt{t}}{l}\right)^2} \tag{4}$$

where the value of t corresponds to time at which $\frac{M_t}{M_\infty} = 0.50$.[26]

Furthermore, the permeability coefficient (P_x) is given by[31]:

$$P_x = D_x \quad S_x \tag{5}$$

where D_x and S_x are the measured diffusion and solubility coefficients for neat polymer (x = p) and nanocomposites (x = nc).

If the measured sorption parameters of neat polymer are known (D_p and S_p), then the solubility ($S_{nc,e}$) and diffusion ($D_{nc,e}$) coefficients of gas in LLDPE/CNC nanocomposites can be estimated theoretically in terms of polymer matrix mass fractions using the following equations[26,27,32–34]:

$$S_{nc,e} = S_p \quad (1 \quad \chi) \tag{6}$$

$$D_{nc,e} = D_p \quad (1 \quad \chi) \tag{7}$$

where S_p and D_p are the solubility and diffusion coefficients of gas in the polymeric matrix and χ is the mass fraction of CNC in the polymer matrix.

3.2 | Tortuosity factor

The gas diffusion coefficients obtained from the sorption experiments can be used to calculate the tortuosity factor, which quantifies the hindrances in the gas diffusion path in the polymer matrix.[35,36] The tortuosity factor (τ) was calculated using the following equation suggested by Bendahou et al[15] and Carrera et al[37]:

$$\tau = \frac{D_p}{D_{nc}} \tag{8}$$

where D_p and D_{nc} correspond to the diffusion coefficients in the pure polymer and nanocomposites, respectively.

3.3 | Gas permeability by isostatic permeability method

The CO_2 and oxygen (O_2) transmission rates of films were measured using the permeability testers Mocon,

Permatran (Model 4/41) and Mocon Ox-Tran (Model 2/21), respectively. The procedures outlined in ASTM D 1434 and ASTM D3985 were used for the testing procedures of CO_2 and O_2 tests, respectively at room temperature (23 ± 0.1 C) and 0% relative humidity (RH). Kurek and coworkers established that the CO_2 and O_2 permeability of polyethylene at 0% RH and 95% RH were of the same order of magnitude.[38] Other researchers also had similar observations for polyethylene suggesting that relative humidity does not have a substantial effect on the gas permeability of polyethylene.[37–41] Thus, the isostatic permeation procedure was carried out at room temperature and 0% RH in this study. For each formulation, a minimum of 3 samples were tested with both gases. The gas permeability (P_{gas}) was calculated using[17,42]:

$$P_{gas} = \frac{GTR\, x\, l}{\Delta P} \tag{9}$$

where GTR is the gas transmission rate, l is the thickness of the film, ΔP is the difference in partial pressure of permeant (carbon dioxide/oxygen) across the sample, which is 101,325 Pa (1 atm).

3.4 | Crystallinity of nanocomposites

Many researchers have estimated the crystallinity of polymers using the Fourier transform infrared spectroscopy (FTIR) for various polymers like polyhydroxy-alkanoates (PHAs),[43] poly (vinyl alcohol),[44] polyethylene,[45] high density polyethylene,[46] polyphenylene sulfide,[47] and so on. Also, the results obtained from the FTIR analysis have been validated with results of calorimetric analysis, showing an excellent correlation between both methods.[47] Consequently, FTIR was employed in this study to quantify the percent crystallinity in bio-LLDPE induced by incorporating CNCs into the matrix.

FTIR spectra of compression molded samples were collected using a Shimadzu IR Affinity IS infrared spectrophotometer (Shimadzu Corporation, Kyoto, Japan) in attenuated total reflectance (ATR) mode. The spectra were obtained with triangle apodization using 64 scans in the range of 4000–400 cm^{-1}, at a wavelength resolution of 4 cm^{-1}.[19,28] Spectra were analyzed by Win FIRST software from Thermo Nicolet (Madison, WI).

The crystallinity of PE is given by[45]:

$$Crystallinity\,(\chi_C) = \frac{I\,(722+730)}{I\,(722+730)+\alpha I(723)} \tag{10}$$

where 'I' corresponds to the infrared intensity for the band at a certain wavenumber, the peaks at 730 and 722 cm^{-1} correspond to crystalline bands whereas the peak at 723 cm^{-1} is associated with amorphous component, and $\alpha = \frac{I^{intr}(722+730)}{I^{intr}(723)}$ corresponds to the ratio of intrinsic crystalline to amorphous band intensities of polyethylene.[45]

FTIR spectra of neat sugarcane LLDPE, CNC, and LLDPE/CNC nanocomposites are illustrated in Figure 1. The main spectral changes are seen in the 1700–500 cm^{-1} frequency range where the peak intensities of absorption bands on the spectrum of LLDPE have significantly decreased by adding CNC into the LLDPE matrix, irrespective of CNC content. Therefore, the spectra were truncated to clearly monitor these changes by comparing spectra of neat LLDPE and nanocomposite with 5% CNC (Figure 2). Both spectra showed two crystalline peaks at 718 and 729 cm^{-1}. Sugarcane-based HDPE also exhibits crystalline peaks at 716–717 cm^{-1}.[6] However, the amorphous peak was not observed at the 723 cm^{-1} for both spectra. Instead, bands associated with the amorphous fraction occurred in the 1400–1250 cm^{-1} region as reported by Hagemann and coworkers.[45] Notice that the intensities of bands at 1400 to 1250 cm^{-1} region assigned to the amorphous component in LLDPE as well as those at 1091–798 cm^{-1} significantly decreased by adding 5% CNC into the matrix (Figure 1). This result suggests a decrease in the amorphous fraction in LLDPE, probably due to the nucleating effect of CNC. Similar trends were observed on the spectra of nanocomposites with other CNC contents in the 1700–500 cm^{-1} region (Figure 1), although not shown in Figure 2. Since the amorphous region of PE was also observed in the frequency range of 1400 to 1250 cm^{-1}, an amorphous peak at 1262 cm^{-1} (Figure 1) was then used to calculate the crystallinity. Consequently, Equation (10) was slightly modified as follows to determine the percent crystallinity of the neat bio-LLDPE and bio-LLDPE in the nanocomposite samples:

$$Crystallinity\,(\chi_C) = \frac{I\,(718+729)}{I\,(718+729)+\alpha\, I(1262)} \tag{11}$$

where $\frac{I^{intr}(718+729)}{I^{intr}(1262)} = 2.18$, as obtained from the measurement specific to this study.

The crystallinity of sugarcane LLDPE in nanocomposites was obtained by performing spectral subtraction. For obtaining the characteristic spectrum of neat LLDPE (i.e., *difference data*) from the spectra of the LLDPE/CNC nanocomposites (i.e., *sample data*), the characteristic spectrum of the cellulose nanocrystal (i.e., *reference data*) was multiplied by the specific percent content of CNCs in the nanocomposite (i.e., *subtraction factor*) for which the crystallinity will be estimated. The obtained spectrum was subtracted from that of its corresponding nanocomposite for which the crystallinity of its component matrix (neat LLDPE) will be determined. Colomw et al performed

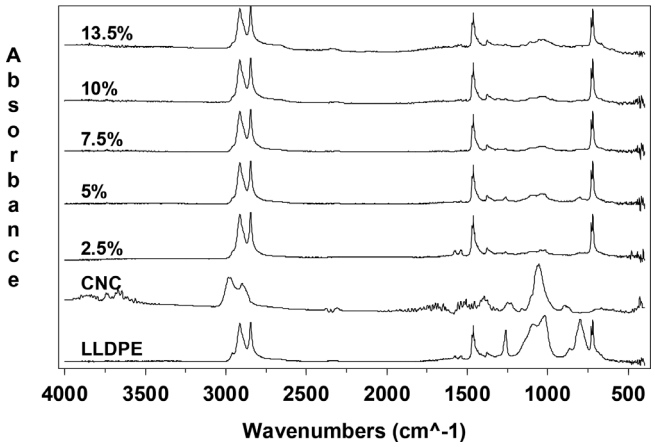

FIGURE 1 FTIR spectra of sugarcane neat LLDPE, CNC, and LLDPE/CNC nanocomposites containing various CNC contents (2.5%–13.5%)

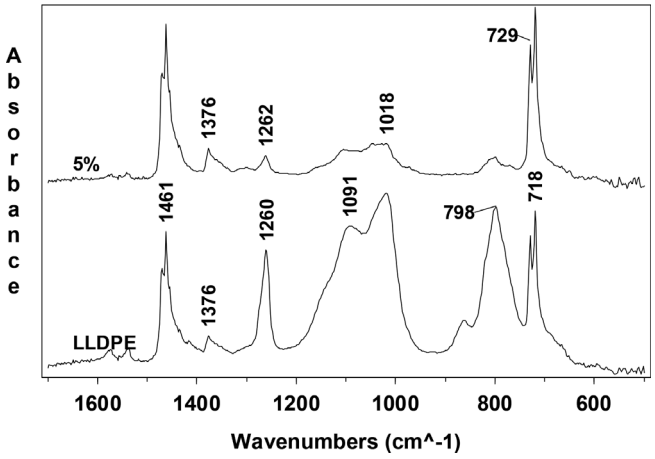

FIGURE 2 Infrared spectra of sugarcane neat LLDPE and LLDPE/5% CNC nanocomposite sheets in the 1700–500 cm^{-1} region

similar procedure for obtaining crystallinity of HDPE from their HDPE/cellulose fiber composites using FTIR.[46] In summary, the following relation was used to extract the characteristic spectrum of neat LLDPE from the spectra of the nanocomposites:

$$Difference\ data = sample\ data \\ (reference\ data\ x\ subtraction\ factor) \quad (12)$$

3.5 | Density measurements

Densities of bio-PEs (LDPE, LLDPE, and HDPE) pellets and LLDPE/CNC nanocomposites were obtained using ColePalmer density gradient apparatus (Cole-Palmer Instrument Company, Vernon Hills, IL). The tests were performed in accordance with the procedure outlined in ASTM D1505-10 (Method C-Continuous filling with liquid entering gradient tube becoming progressively more dense) by observing the level to which a test specimen sinks in a liquid gradient column. The density gradient column was prepared using high pressure liquid chromatography (HPLC)-grade water (750 ml) and isopropanol (500 ml) of densities 0.79 and 1 g/cm^3, respectively.

3.6 | Optical microscopy and light transparency

Microscope image of bio-LLDPE and bio-LLDPE/CNC nanocomposites were obtained at 12.5 magnification using an Olympus BX41 optical microscope (Olympus, Center Valley, PA) equipped with a camera (Olympus Qcolor3). Microscope images of films were obtained directly from the manufactured ~0.062 mm thick films. On the other hand, the 2 mm thick compression molded samples were compressed further to reduce its thickness to allow light transmission through the sample while capturing images.

The transparency of LLDPE and LLDPE/CNC nanocomposite films was recorded over a wavelength range of 200–900 nm at a scan rate of 340 nm/min in duplicate using a ultraviolet–visible spectrophotometer Perkin-Elmer Lambda 25 (Perkin-Elmer Instruments, Beaconsfield, UK).[17,19] For each spectrum, the percent light transmission value reported was at 550 nm, which is the mid-point in the visible light range (~380–720 nm).[17,19]

3.7 | Statistical analysis

A one-way *t* tests with an α of 0.05 were conducted to compare the permeability coefficients obtained from two different permeability testing methods (isostatic permeability method versus gravimetric method) and three different bio-PE types (LDPE, LLDPE, and HDPE). Similar *t* tests were done to assess the effect of CNC content on the crystallinity, diffusion coefficient, solubility coefficient, light transparency, and permeability coefficient of bio-LLDPE.

4 | RESULTS AND DISCUSSION

4.1 | Effect of testing methods (isostatic versus gravimetric) on CO_2 permeability of PE

Numerous methods, including a gravimetric technique and an isostatic permeation procedure, have been

TABLE 1 Effect of testing method on the carbon dioxide permeability (P_{CO2}) of various bio-PE grades

	Density of pellets (g/cm^3)			P_{CO2} (10^{17} kg m/m^2 s Pa)		
Bio-PE types	**Provided**	**Measured**	**Literature[a]**	**Isostatic[b]**	**Gravimetric[b]**	**Literature[a]**
LLDPE	0.916	0.915 ± 0.001	0.916–0.940 [8]	27.9 ± 0.70^A	29.3 ± 1.74^A	31.9 [49]
LDPE	0.924	0.919 ± 0.001	0.910–0.925 [8]	—	22.9 ± 0.4	17 to 24 [8]
HDPE	0.962	0.951 ± 0.001	0.940–0.965 [8]	8.28 ± 0.4^B	8.02 ± 0.42^B	10.09 [37]

[a]Listed values are for petroleum-based polymers and superscript numbers represent the cited references.
[b]Similar superscript letters indicate that the difference in the two-treatment means is not significant based on the *t* test results at a 5% significance level.

employed for measuring the permeation parameters of various permeants through polymers. Gravimetric permeation is a simple and straight forward method since it allows one to directly calculate both the solubility at steady state (S) and diffusion (D) coefficients from the sorption/desorption curve, from which the permeability (P) coefficient is calculated using Equation 5. Conversely, the isostatic permeation procedure involves calculation of P at steady state, with D obtained from the transient state portion of the permeability experiment's flux rate profile curve. Once P and D are obtained, then S (transient state) is calculated using Equation 5.[15,31,42] Since the gravimetric approach was selected in this study, the permeability coefficient values determined by these two procedures for the same PE/CO_2 system was compared to validate the selected permeation method.

Table 1 lists the CO_2 permeability coefficients of three types of bio-PE determined by a gravimetric procedure and an isostatic permeability technique. Interestingly, the permeability coefficients obtained by the two methods were similar and no statistically significant difference was observed between the two methods, irrespective of PE grade. However, the CO_2 permeability was affected by the PE grade, LLDPE showing the highest coefficient permeability and HDPE the lowest. Such a trend was expected and attributed to the difference in density of these three PE (Table 1). LLDPE with the lowest density had the highest permeability followed by LDPE and HDPE. The density is approximately inversely proportional to the free volume of the polymer and proportional to the crystallinity of the polymer.[48] Polymers with lower density have poor chain packing and lower crystallinity. Hence, it can be inferred that LLDPE having the lowest density (Table 1) would have the highest free volume leading to a higher permeability value. Wang and coworkers studied the effect of polyethylene density on gas permeability and reported similar trends.[48] Their results indicated that the permeability of polyethylene decreases by a factor of almost 5–6 for an approximate increase of 5% in density.[48] It is worth mentioning that the CO_2 permeability values of different PE determined by both methods are in accordance with the values reported in the literature (Table 1),[8,37,49] suggesting that that both methods are equally reliable techniques to measure the permeability of polymers. However, the gravimetric method was chosen for further investigation as this method can be used to easily obtain the diffusion coefficient needed to quantify the tortuosity effect in LLDPE/CNC nanocomposites.

4.2 | CO_2 barrier improvement and its mechanisms in LLDPE/CNC nanocomposite sheets

4.2.1 | Effect of CNC addition on the crystallinity of LLDPE

The crystallinity of LLDPE from the spectra of the LLDPE/CNC nanocomposites obtained by the infrared spectra subtraction method was determined to establish correlation between crystallinity and permeability coefficients. The crystallinity of LLDPE increased with CNC addition level up to 2.5% and remained constant as the CNC content increased further (Table 2). The increased crystallinity can be attributed to the highly crystalline CNCs acting as an effective nucleating agent.[17,18,50] It should be mentioned that all nanocomposites had similar percent crystallinities since the addition of more than 2.5% CNCs did not improve LLDPE crystallinity further probably due to the retarded crystal growth caused by CNC agglomerations at high loading levels.[17,18] A loading level of 2.5% CNC or probably lower appeared to be the maximum concentration of CNC for an effective heterogeneous crystal nucleation in LLDPE matrix. Karkhanis and coworkers reported similar nucleating effect when CNCs were added to PLA matrix.[17] A maximum increase in PLA crystallinity was observed at 1% CNC content in their study and further addition of CNCs to the PLA matrix did not affect the crystallinity.[17] This is in general agreement with the results of Clarkson and coworkers who recently reported similar trends where very small concentrations of CNC (0.05 and 0.55 wt%) are found effective heterogeneous nucleation agent for PLAs.[50]

TABLE 2 Effect of CNC content on the crystallinity (χ), density, and CO_2 permeation parameters of compression molded bio-LLDPE sheet measured by gravimetric method

CNC content (%)	% χ^a	Density (g/cm^3)	Diffusion[a] (10^{-7} cm^2/s)		Tortuosity factor (%)	Solubility[a] (10^{-4} g/m^3 Pa)		P_{CO2}[a] (10^{-17} kg m/m^2 s Pa)	Percent decrease in P_{CO2}
			Experimental (D_x)	Predicted ($D_{nc,e}$)		Experimental (S_x)	Predicted ($S_{nc,e}$)	(P_x)	
0	50.0 ± 0.0^A	0.920 ± 0.001	5.2 ± 0.4^A	5.2	100	57.2 ± 1.7^A	57.2	29.3 ± 1.74^A	—
2.5	73.7 ± 1.4^B	0.925 ± 0.002	4.9 ± 0.2^{AB}	5.1	107 ± 5.0	54.3 ± 0.9^{AB}	52.9	26.6 ± 1.3^A	9
5	73.0 ± 0.5^B	0.933 ± 0.002	4.6 ± 0.2^{BC}	4.9	114.1 ± 4.7	57.1 ± 0.6^{AB}	54.2	26.3 ± 1.1^{AB}	10
7.5	75.3 ± 0.6^B	0.944 ± 0.002	4.3 ± 0.1^C	4.8	120.8 ± 3.4	53.1 ± 1.0^{BC}	49.1	23.0 ± 0.9^B	22
10	75.3 ± 0.4^B	0.950 ± 0.005	3.7 ± 0.2^D	4.7	143.9 ± 9.6	50.4 ± 1.6^C	45.4	18.7 ± 1.3^C	36
13.5	74.1 ± 0.8^B	—	3.5 ± 0.1^D	4.5	147.2 ± 2.6	55.5 ± 1.1^{AB}	48.0	19.6 ± 0.4^C	33

[a]Similar superscript letters in each column are not significantly different based on the *t* test results at a 5% significance level.

Other researchers also validated this trend; with the addition of about 1% CNC into the polymer matrix showing improvement in crystallinity, which remained constant thereafter.[18–21]

4.2.2 | Effect of CNC addition on the CO_2 diffusion and solubility coefficients of LLDPE

Table 2 summarizes the experimentally measured CO_2 diffusion (D_x) and solubility (S_x) as well as calculated permeability (P_x) coefficients of LLDPE and LLDPE/CNC nanocomposites. The $S_{nc,e}$ and $D_{nc,e}$ coefficients predicted from Equations 6 and 7, respectively, are also listed. The experimental diffusion coefficient decreased almost linearly as the CNC content increased in the nanocomposites and this reduction was statistically significant (p-value <0.0001). Similar trend was obtained for the $D_{nc,e}$ coefficient predicted from Equation 7. In contrast, the experimental solubility coefficient remained almost constant as the CNC content increased in the nanocomposites. This trend did not corroborate the one predicted from Equation 6 due to a probable gas loss, which is unavoidable, during weight gain measurements in a batch sorption process.[27] Nevertheless, the theoretically predicted $D_{nc,e}$ coefficients were slightly higher and that predicted $S_{nc,e}$ coefficients were slightly lower than the experimental ones. The discrepancy between the measured and predicted values increased with CNC content. This could be due to not taking into consideration in Equations 6 and 7 the mass fraction of crystals available in LLDPE, which is a semi crystalline polymer. A poor adhesion between the polymer matrix and cellulosic fibers in composites without coupling/compatibilizer agent also contributes to the difference between the measured and predicted gas sorption parameters in cellulose-based composites.[27]

Reductions in D_x and/or S_x coefficients were expected since these sorption parameters are a function of the polymer matrix mass fraction in the composites.[26,27,32–34,51] Our previous work on cellulosic fiber/plastic composites demonstrated that cellulose fibers reject gas by acting like crystallites, and only the amorphous region in the composite (i.e., polymer matrix) absorbs the gas.[26,27] Not only increasing the fiber contents into the composites reduces the matrix mass fraction available for gas diffusion in the composite, but also the fiber regions in the composites obstruct the movement of gas molecules and, therefore, increase the average length of the paths they must travel.[26,27] Thus, the diffusion (D_x) coefficient decreased as the polymer mass fraction decreased in the nanocomposites and that the addition of CNCs increased the CO_2 diffusion time in the nanocomposites, in good

agreement with results reported by other investigators.[15,22–24,36] Unfortunately, the decrease in the solubility (S_x) of CO_2 in LLDPE/CNC nanocomposites as predicted by Equation 6 was not observed in this study as previously explained.

4.2.3 | Correlations between crystallinity, tortuosity factor, and permeability coefficient

Table 2 summarizes the CO_2 permeability (P_x) coefficients and tortuosity factors of LLDPE calculated from Equations 5 and 8, respectively, as a function of CNC contents. As, expected the P_{CO2} coefficients of LLDPE decreased as the CNC content increased due to the decrease in D_x coefficient as discussed above. This indicates that the permeation process was partly controlled by diffusion through the LLDPE matrix. The addition of CNC significantly improved the CO_2 barrier performance of LLDPE sheet up to 10 wt% content and leveled off above this concentration.

Remarkably, though the crystallinity of bio-LLDPE increased with CNC content up to 2.5% and remained constant thereafter, the CO_2 permeability coefficient in the nanocomposites on the other hand decreased almost linearly with increasing amounts of CNCs (Table 2). This suggests that the crystallization of LLDPE matrix caused a decrease of CO_2 permeability but not in linear proportion with the decrease in amorphous volume and that the gas permeability in LLDPE appeared to be controlled by other factors in addition to level of crystallinity. In other terms, even though the polymer crystallinity played a role in improving the CO_2 barrier property of bio-LLDPE up to 2.5% CNC, it is certainly not the only factor influencing its gas barrier improvement above this CNC addition level. Our results are in good agreement with those of other investigators who reported no correlation between percent crystallinity and permeability coefficient.[22–24] Indeed, Frounchi and coworkers observed a two-fold reduction in both oxygen and carbon dioxide permeability coefficients of the PP/EPDM blend filled with 1.5 vol% organoclay compared to unfilled PP/EPDM blend, despite a 27% reduction in nanocomposite crystallinity.[22] Similar results have also been observed by other researchers.[23,24] A significant decline in both O_2 (about 45%) and CO_2 (about 68%) permeability coefficients of PLA films was obtained by adding 1.37 vol% graphene oxide nanosheets into PLA film, even though all the PLA nanocomposite films were basically amorphous.[23] Therefore, in addition to level of crystallinity and/or crystal morphology, the role of other factors contributing to barrier improvement like the tortuosity factor must also be investigated to understand the mechanisms of barrier improvement in nanocomposites.

Since the CO_2 permeation process (decreased permeability coefficient) in the nanocomposite was partly controlled by the gas diffusion through the LLDPE matrix, the observed decrease in diffusion coefficient in the nanocomposites indicated an increase in the gas diffusion time as per Equation (4). The increased diffusion time was attributed to the CNCs acting as impermeable crystals for the movement of gas molecules through the polymer matrix creating a tortuous path for the movement of gas molecules. This mechanism known as a tortuosity effect is illustrated in Figure 3 showing a path A that represents the semi-crystalline polymer matrix without CNCs and a path B representing the counterpart with CNCs. The diffusion time in path B will be greater than in path A due to the presence of CNCs, which creates a tortuous path for the movement of gas molecules; thus increasing its diffusion time. Huang and coworkers attributed the improved gas barrier performance of PLA/graphene oxide nanosheets to the tortuosity effect created by the impermeable graphene oxide

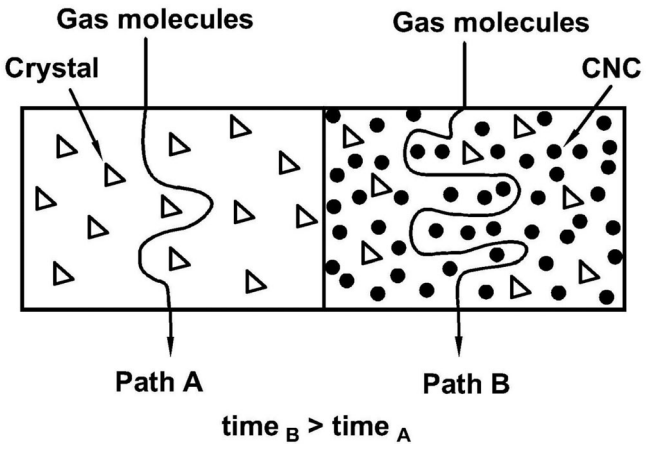

FIGURE 3 Schematic diagram of the proposed tortuosity effect in a semi-crystalline plastic

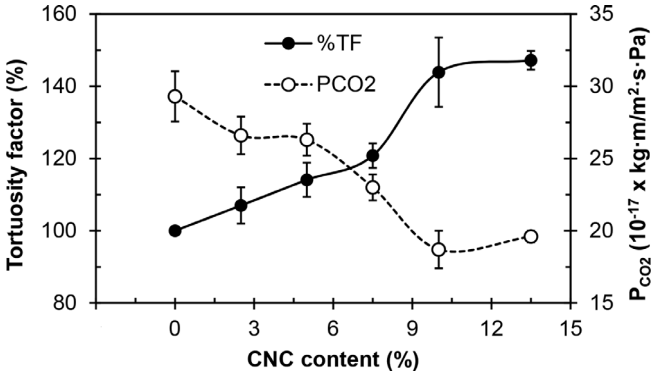

FIGURE 4 Effect of CNC content on tortuosity factor (TF) and carbon dioxide permeability coefficient (P_{CO2}) of bio-LLDPE

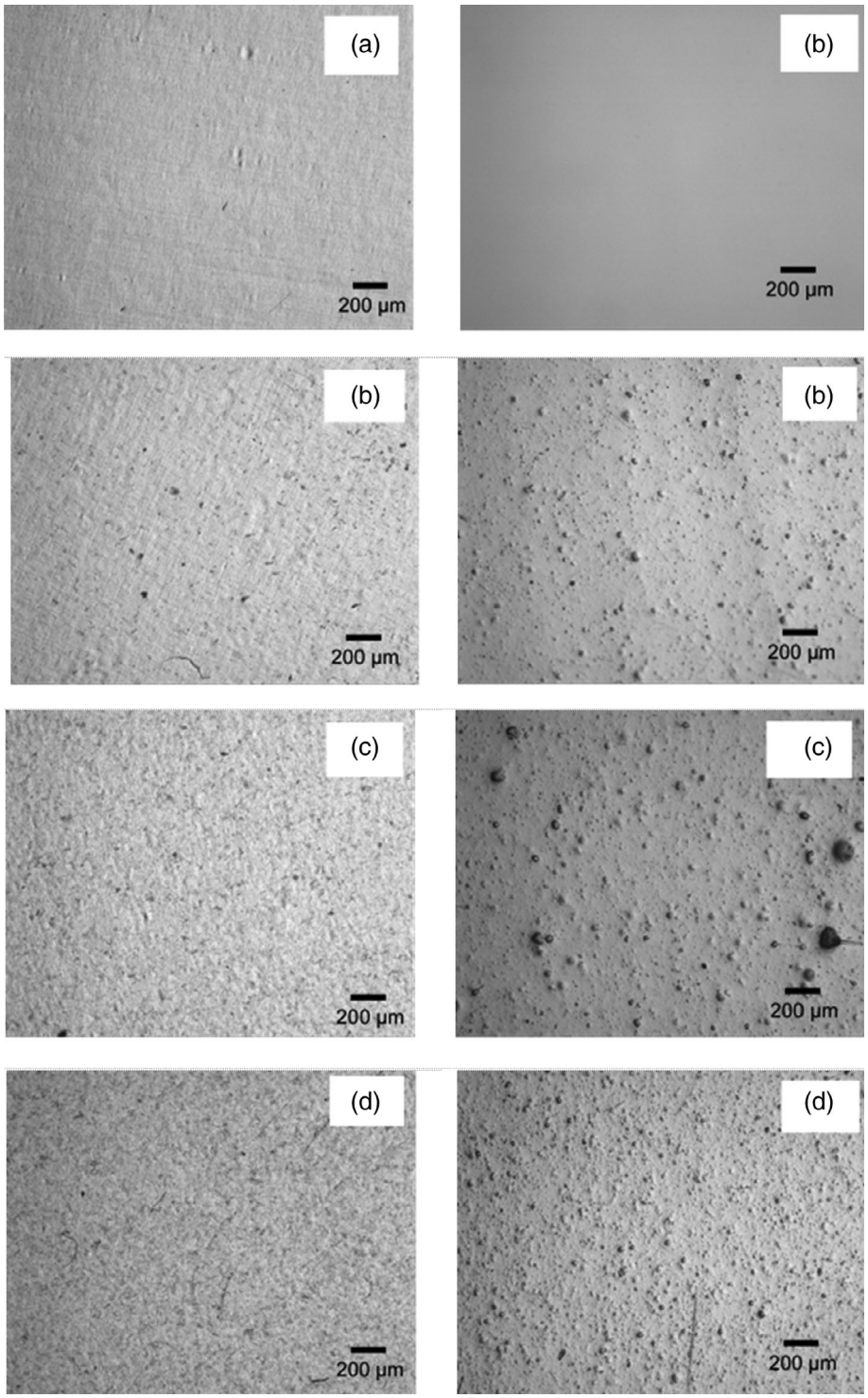

FIGURE 5 Optical microscope images of bio-LLDPE sheets (left column) with various CNC contents: (a) 0%; (b) 2.5%; (c) 7.5%; and (d) 13.5% as well as of bio-LLDPE films (right column) with various CNC contents: (a) 0%; (b) 1%; (c) 2.5%; and (d) 3.5%

nanosheets.[23] Likewise, numerous investigators have claimed this tortuosity mechanism to explain improvement in gas and/or water vapor barrier of various polymers[22,24] but without quantifying it.

In this study, the tortuosity effect was quantified as the tortuosity factor according to Equation (8) (Table 2). The effect of CNC content on the tortuosity factor and CO_2 permeability coefficient is illustrated in Figure 4. The estimated tortuosity factor increased with the increase of CNC content in the nanocomposites. This result was expected since CNCs obstruct the movement of gas molecules in the nanocomposites, then more CNCs in the nanocomposites tend to increase the average length of the paths the gas molecule must travel in the sample; thus, increasing the tortuosity factor. Moreover, samples of nanocomposite sheets and films with various

TABLE 3 Effect of CNC addition on the light transparency as well as CO_2 and O_2 permeability of bio-LLDPE films measured by isostatic method

LLDPE composition	Light transmission at 550 nm (%)[a]	Gas permeability (10^{-17} kg m/m^2 s Pa)[a]			
		P_{CO2}	% Decrease in P_{CO2}	P_{O2}	% Decrease in P_{O2}
Control	56.0 ± 2.1^{A}	27.9 ± 0.70^{A}	—	31.8 ± 2.27^{A}	—
1% CNC	55.2 ± 0.3^{A}	25.1 ± 1.23^{B}	10	24.5 ± 1.29^{B}	23
2.5% CNC	46.8 ± 0.9^{B}	18.7 ± 2.77^{C}	33	16 ± 0.72^{C}	50

[a]Different superscript letters in each column indicate that the difference is statistically significant at values of "Prob>|t|" less than 0.05.

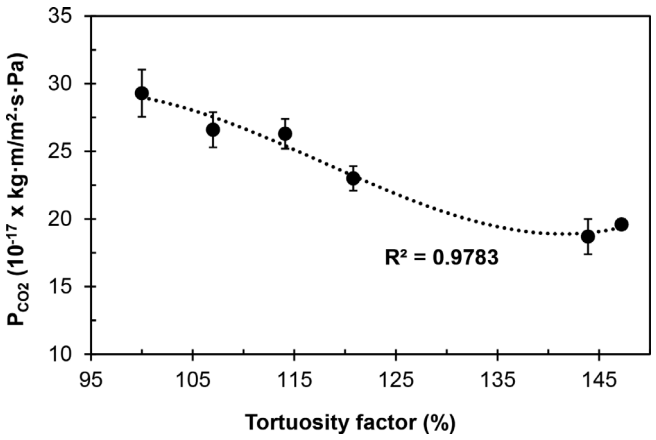

FIGURE 6 Carbon dioxide permeability coefficient (P_{CO2}) versus tortuosity factor

CNC contents were observed under an optical microscope to illustrate the tortuosity effect (Figure 5). The images showed an increase in the number of CNC particles present per unit area with increase in concentration of CNC; thus, the more CNC in the material, the higher is the tortuosity factor. The CO_2 permeability coefficient of LLDPE decreased almost linearly with increasing amounts of CNCs as previously discussed (Table 2 and Figure 4).

Indeed Figure 5 shows CNC agglomeration due to limited CNC dispersion in the matrix at higher loading levels. It is worth mentioning that the dispersion of CNC in LLDPE sheet (Figure 5(b)-(d) on the left) was different than in the film counterparts (Figure 5(b)-(d) on the right) probably due to the difference in processing techniques used to manufacture these samples. Since the agglomeration issue has been discussed in detail in our previous work on PLA/CNC films,[17,19] this phenomenon was not discussed in this paper because our intent was just to illustrate the increased number of particles as CNC content increased in the matrix.

Nevertheless, it is important to mention that light transparency can be used as an indicator of the dispersion of nanoparticles in a matrix, if the size of individual nanoparticles is smaller than the wavelength of visible light (380–720 nm).[19] Karkhanis and coworkers have reported that the addition of CNCs into a polymeric matrix does not affect the transparency of resulting films if nanosize dispersion of CNC in the matrix is achieved, because pure CNC films are highly transparent.[17,19] The experimental results showed that the light transmission of neat LLDPE decreased significantly by adding 2.5% CNCs (Table 3); implying that nanoscale dispersion did not fully occur and some micrometer sized agglomerations were still present, in agreement with the images shown in Figure 5. The presence of these micrometer-sized CNC agglomerations larger than the incident wavelength of light (nanometer) in the nanocomposite films scatters light, thus reducing film transparency.[17,19]

A strong negative correlation was established between the tortuosity factor and the permeability coefficient. As the tortuosity factor increased the CO_2 permeability coefficient values decreased (Figure 6). This correlation showed a good fit with an R^2 value (order 3 polynomial regression) of approximately 98% (Figure 6), clearly indicating that factors other than crystallinity also contribute to gas barrier improvement of polymers.

4.3 | CO_2 and O_2 barrier properties of LLDPE films with CNCs

LLDPE is used in many flexible packaging applications like heavy duty shipping sacks, stretch/cling film, grocery snacks, and so on. Hence, it is important to investigate the effect of CNCs addition on the gas barrier of bio-LLDPE films, in addition to the nanocomposite sheets discussed previously. The films were studied for their oxygen and carbon dioxide barrier properties, the most important gases crucial for food packaging applications, to understand the effect of CNC addition on LLDPE gas barrier enhancement (Table 3).

As expected, a significant reduction in gas permeability coefficients of bio-LLDPE films was obtained by adding CNCs into the matrix. Both the CO_2 and O_2 permeability

coefficients of LLDPE significantly decreased by about 33% and 50%, respectively, by adding only 2.5% CNC. The enhanced gas barrier performance of bio-LLDPE/CNC films are mainly assigned to the efficient nucleating effect of CNCs in the bio-LLDPE matrix along with the tortuosity effect created by the impermeable CNC crystals for the movement of gas molecules. The microscope images in Figure 5 clearly show an increase in the number of CNC particles present per unit area with increase in concentration of CNC, confirming the tortuosity effect. Several studies have reported similar nucleating effect on addition of CNCs to the polymer matrix.[17,18] Furthermore, these results also validate the gas barrier enhancement results achieved in the nanocomposites sheets discussed previously.

Interestingly, the film samples required less amount of CNCs to show a similar improvement in CO_2 barrier as compared to the nanocomposite sheets. The reason for this is unclear now but this could be ascribed to the bi-directionally stretched blown extrusion film having different kinds of crystalline structures compared to uniaxially-stretched compression molding sheets. The voids in compression molded samples could also account for this discrepancy. However, this hypothesis was ruled out since the density of LLDPE/CNC nanocomposites increased with CNC content (Table 2) as expected from the rule of mixtures due to the higher specific gravity of CNC (~1.45) compared to that of LLDPE. The density of compression molded LLDPE increased from 0.920 to 0.950 g/cm^3 by adding 10% CNC into the matrix. The nanocomposite sank to the bottom of the column at 13.5% CNC; thus, no value was collected at this concentration (Table 2).

5 | CONCLUSIONS

This study was intended at improving the gas barrier property of sugarcane based LLDPE using cellulose nanocrystals (CNCs). Specifically, this study evaluated the effect of testing methods (isostatic versus gravimetric) on CO_2 permeability of various bio-PE grades as well as the effect of CNC content on crystallinity, tortuosity factor, and gas barrier properties of bio-LLDPE sheets and films.

The isostatic and gravimetric permeation methods yielded similar CO_2 permeability coefficients irrespective of bio-PE grade (LLDPE, LDPE, and HDPE), making both methods equally reliable to measure the gas permeability of the polymers. The density of bio-PE negatively correlated with the CO_2 permeability coefficient. The crystallinity of bio-LLDPE increased with CNC addition level up to 2.5% and remained constant as the CNC content increased further attributable to the crystal nucleating effect of CNC and the retarded crystal growth caused by CNC agglomerations at high loading levels, respectively. The CO_2 diffusion coefficient in bio-LLDPE decreased almost linearly as the CNC content increased because the addition of CNC decreased the mass fraction of polymer available for gas diffusion and increased the CO_2 diffusion time in the nanocomposites. As a result, the CO_2 permeability coefficient of LLDPE also decreased almost linearly with increasing CNC content. A significant decline in CO_2 (about 36%) permeability coefficients (P_{CO2}) of LLDPE sheets was obtained by adding 10 wt% of CNCs into LLDPE sheet, and P_{CO2} values leveled off above this concentration. No correlation was established between gas permeability and percent crystallinity of LLDPE sheet since the permeability coefficient decreased almost linearly with increasing CNC content whereas the crystallinity of the nanocomposites increased only up to 2.5% CNC content and remained constant thereafter. In contrast, a strong negative correlation was established between the tortuosity factor and the permeability coefficient, clearly indicating that factors other than percent crystallinity also contribute to gas barrier improvement of bio-LLDPE. The effect of CNC addition on the gas barrier properties of bio-LLDPE films was also examined. As expected, a significant improvement in gas barrier of bio-LLDPE films was obtained by adding CNCs into the matrix. The P_{CO2} and P_{O2} coefficients of bio-LLDPE films reduced by 33% and 50%, respectively, when 2.5% of CNC was added into the films, validating the gas barrier enhancement results achieved with nanocomposites sheets. This study provides a significant guidance for using biobased green LLDPE in a wide range of packaging applications due to its improved gas barrier properties.

ACKNOWLEDGMENTS

We gratefully acknowledge McIntire-Stennis, Project # 1017725 for financial support of this research work.

ORCID

Laurent M. Matuana https://orcid.org/0000-0002-5645-7451

REFERENCES

[1] R. C. Thompson, C. J. Moore, F. S. Vom Saal, S. H. Swan, *Philos. Trans. R. Soc. Lond., B Biol. Sci.* **2009**, *364*, 2153.
[2] T. Iwata, *Angew. Chem., Int. Ed.* **2015**, *54*, 3210.
[3] J. Boonniteewanich, S. Pitivut, S. Tongjoy, S. Lapnonkawow, S. Suttiruengwong, *Energy Procedia* **2014**, *56*, 518.
[4] O. Türünç, L. Montero de Espinosa, M. A. R. Meier, *Macromol. Rapid Commun.* **2011**, *32*, 1357.
[5] Bioplastics market size, share & trends analysis report by product, by production technology, regional outlook, competitive strategies, and segment forecasts, 2019 to 2025 accessed December 29 2020.

[6] P. Bazan, P. Nosal, B. Kozub, S. Kuciel, *Materials* **2020**, *13*, 2967.
[7] A. Emblem, in *Packaging Technology: Fundamentals, Materials and Processes* (Eds: A. Emblem, H. Emblem), Woodhead Publishing, Philadelphia, Pennsylvania, USA **2012**, p. 287.
[8] S. E. Selke, J. D. Culter, *Plastics Packaging: Properties, Processing, Applications, and Regulations*, Hanser, Cincinnati, Ohio, USA **2016**.
[9] E. Kontou, M. Niaounakis, *Polymer* **2006**, *47*, 1267.
[10] H. Ashizawa, J. E. Spruiell, J. L. White, *Polym. Eng. Sci.* **1984**, *24*, 1035.
[11] A. G. Erlat, R. J. Spontak, R. P. Clarke, T. C. Robinson, P. D. Haaland, Y. Tropsha, N. G. Harvey, E. A. Vogler, *J. Phys. Chem. B.* **1999**, *103*, 6047.
[12] P. Dole, L. Averous, C. Joly, G. Della Valle, C. Bliard, *Polym. Eng. Sci.* **2005**, *45*, 217.
[13] J. Wang, D. J. Gardner, N. M. Stark, D. W. Bousfield, M. Tajvidi, Z. Cai, *ACS Sustainable Chem. Eng.* **2018**, *6*, 49.
[14] C. M. O. Müller, J. B. Laurindo, F. Yamashita, *Ind. Crop Prod.* **2011**, *33*, 605.
[15] A. Bendahou, H. Kaddami, E. Espuche, F. Gouanvé, A. Dufresne, *Macromol. Mater. Eng.* **2011**, *296*, 760.
[16] M. Jonoobi, J. Harun, A. P. Mathew, K. Oksman, *Compos. Sci. Technol.* **2010**, *70*, 1742.
[17] S. S. Karkhanis, N. M. Stark, R. C. Sabo, L. M. Matuana, *Compos. Part A Appl. Sci. Manuf.* **2018**, *114*, 204.
[18] Y. Liu, L. M. Matuana, *J. Appl. Polym. Sci.* **2019**, *136*, 47594.
[19] S. S. Karkhanis, N. M. Stark, R. C. Sabo, L. M. Matuana, *Polym. Eng. Sci.* **2018**, *58*, 1965.
[20] E. Fortunati, M. Peltzer, I. Armentano, L. Torre, A. Jiménez, J. M. Kenny, *Carbohydr. Polym.* **2012**, *90*, 948.
[21] M. D. Sanchez-Garcia, J. M. Lagaron, *Cellulose* **2010**, *17*, 987.
[22] M. Frounchi, S. Dadbin, Z. Salehpour, M. Noferesti, *J. Membr. Sci.* **2006**, *282*, 142.
[23] H. D. Huang, P. G. Ren, J. Z. Xu, L. Xu, G. J. Zhong, B. S. Hsiao, Z. M. Li, *J. Membr. Sci.* **2014**, *464*, 110.
[24] M. Drieskens, R. Peeters, J. Mullens, D. Franco, P. J. Lemstra, D. G. Hristova-Bogaerds, *J. Polym. Sci., Part B: Polym. Phys.* **2009**, *47*, 2247.
[25] N. M. Stark, *J. Renewable Mater.* **2016**, *4*, 313.
[26] L. M. Matuana, F. Mengeloglu, J. Vinyl, *Addit. Technol.* **2001**, *7*, 67.
[27] L. Matuana-Malanda, C. B. Park, J. J. Balatinecz, *J. Cell Plast.* **1996**, *32*, 449.
[28] S. S. Karkhanis, L. M. Matuana, *Polym. Eng. Sci.* **2019**, *59*, 2211.
[29] J. Crank, *The Mathematics of Diffusion*, Oxford University Press, London, UK **1979**.
[30] M. G. De Angelis, in *Encyclopedia of Membranes* (Eds: E. Drioli, L. Giorno), Springer, Berlin/Heidelberg, Germany **2014**, p. 62.
[31] C. D. Barr, J. R. Giacin, R. J. Hernandez, *Packag. Technol. Sci.* **2000**, *13*, 157.
[32] D. W. Van Krevelen, *Properties of Polymers*, Elsevier, New York, USA **1990**.
[33] A. S. Michaels, H. J. Bixler, *J. Polym. Sci.* **1961**, *50*, 393.
[34] A. S. Michaels, H. J. Bixler, *J. Polym. Sci.* **1961**, *50*, 413.
[35] J. A. Horas, M. G. Rizzotto, in *Polypropylene: An A-Z Reference*, Vol. 2 (Ed: J. Karger-Kocsis), Springer, Netherlands **1999**, p. 273.
[36] V. Compañ, L. F. Del Castillo, S. I. Hernandez, M. M. Lopez-Gonzalez, E. Riande, *J. Polym. Sci., Part B: Polym. Phys.* **2010**, *48*, 634.
[37] M. C. Carrera, E. Erdmann, H. A. Destéfanis, *J. Chem.* **2013**, *2013*, 679567.
[38] M. Kurek, M. Ščetar, A. Voilley, K. Galic, F. Debeaufort, *J. Membr. Sci.* **2012**, *403*, 162.
[39] M. Kurek, A. Guinault, A. Voilley, K. Galic, F. Debeaufort, *Food Chem.* **2014**, *144*, 9.
[40] N. H. Ullsten, M. S. Hedenqvist, *Polym. Test.* **2003**, *22*, 291.
[41] M. A. Osman, A. Atallah, *Macromol. Rapid Commun.* **2004**, *25*, 1540.
[42] G. D. Dimitroulas, A. B. Badeka, M. G. Kontominas, *Polym. J.* **2004**, *36*, 198.
[43] M. Kansiz, A. Domínguez-Vidal, D. McNaughton, B. Lendl, *Anal. Bioanal. Chem.* **2007**, *388*, 1207.
[44] O. N. Tretinnikov, S. A. Zagorskaya, *J. Appl. Spectrosc.* **2012**, *79*, 521.
[45] H. Hagemann, R. G. Snyder, A. J. Peacock, L. Mandelkern, *Macromolecules* **1989**, *22*, 3600.
[46] X. Colomw, J. Canavate, P. Pagés, J. Saurina, F. Carrasco, *J. Reinf. Plast. Compos.* **2000**, *19*, 818.
[47] K. C. Cole, D. Noël, J. J. Hechler, D. Wilson, *Microchim. Acta* **1988**, *94*, 291.
[48] Y. Wang, A. J. Easteal, X. D. Chen, *Packag. Technol. Sci.* **1998**, *11*, 169.
[49] N. Euaphantasate, P. Prachayawasin, S. Uasopon, P. Methacanon, *J. Met. Mater. Miner.* **2008**, *18*, 103.
[50] C. M. Clarkson, S. M. El Awad Azra, G. T. Schueneman, J. F. Snyder, J. P. Youngblood, *Polymer* **2020**, *187*, 122101.
[51] L. Matuana, Q. Li, *Cell. Polym.* **2001**, *20*, 115.

How to cite this article: M. Natarajan, R. C. Sabo, N. M. Stark, L. M. Matuana, *J. Appl. Polym. Sci.* **2022**, *139*(3), e51515. https://doi.org/10.1002/app.51515